### Title
Targeted excision of VCP R155H mutation by Cre-LoxP technology as a promising therapeutic strategy for valosin-containing protein disease.




### Journal
Human Gene Therapy Clinical Development, 26(1)



### Authors
Nalbandian, Angèle
Llewellyn, Katrina
Nguyen, Christopher
et al.



### Publication Date
2015-02-01

### DOI
10.1089/hgtb.2014.096

Peer reviewed

HUMAN GENE THERAPY METHODS 26:13–24 (February 2015)

DOI: 10.1089/hgtb.2014.096

# Targeted Excision of VCP R155H Mutation by Cre-*LoxP* Technology as a Promising Therapeutic Strategy for Valosin-Containing Protein Disease

Angèle Nalbandian,[1] Katrina J. Llewellyn,[1] Christopher Nguyen,[1] Edward S. Monuki,[2] and Virginia E. Kimonis[1]

**Abstract**

Inclusion body myopathy associated with Paget's disease of the bone and frontotemporal dementia is attributed to mutations in the valosin-containing protein (*VCP*) gene, mapped to chromosomal region 9p13.3–12. Affected individuals exhibit scapular winging and die from progressive muscle weakness and cardiac and respiratory failure in their 40s to 50s. Mutations in the *VCP* gene have also been associated with amyotrophic lateral sclerosis in 10–15% of individuals with hereditary inclusion body myopathy and 2–3% of isolated familial amyotrophic lateral sclerosis. Currently, there are no effective treatments for VCP-related myopathy or dementia. To determine the effects of targeted excision of the most common R155H mutation in VCP disease, we generated the Cre-ER$^{TM}$-VCP$^{R155H/+}$ tamoxifen-inducible model. We administered tamoxifen (0.12 mg/g body weight) or corn oil (vehicle) to the pregnant dams by oral gavage and monitored survival and muscle strength measurements of the pups until 18 months of age. We confirmed efficient removal of exons 4 and 5 and recombination of the mutant/floxed VCP copies by Q-PCR analyses. The activity and specificity of Cre recombinase was confirmed by immunostaining. Herein, we report that Cre-ER$^{TM}$-VCP$^{R155H/+}$ mice demonstrated improved muscle strength and quadriceps fibers architecture, autophagy signaling pathway, reduced brain neuropathology, decreased apoptosis, and less severe Paget-like bone changes. The Cre-ER$^{TM}$-VCP$^{R155H/+}$ mouse model provides proof of principle by demonstrating that removal of the mutated exons could be beneficial to patients with VCP-related neurodegenerative diseases, and serves as an excellent platform in understanding the underlying pathophysiological mechanism(s) in the hopes of a promising therapeutic approach.

## Introduction

Inclusion body myopathy associated with Paget's disease of the bone (PDB) and frontotemporal dementia (OMIM 167320) was first reported in 2000 by Kimonis et al.,[1] mapped to the human chromosomal region 9p13.3–12.[2,3] In 2004, the disease was attributed to being caused by mutations in the gene encoding valosin-containing protein (VCP).[4] Classic symptoms of VCP disease include weakness and atrophy of the pelvic and shoulder girdle muscles in 90% of individuals.[1–3] Affected individuals exhibit scapular winging and die from progressive muscle weakness, and cardiac and respiratory failure, typically in their 40s to 50s.[1,5] Histologically, patients show the presence of rimmed vacuoles and TAR DNA-binding protein 43 (TDP-43)-positive ubiquitinated inclusion bodies in the muscles.[1,4–6] The variable phenotype is often diagnosed as limb girdle muscular dystrophy, amyotrophic lateral sclerosis (ALS), facioscapular muscular dystrophy, or scapuloperoneal muscular dystrophy.[5,7,8] To date, 31 *VCP* mutations have been reported in families from several parts of the world, including Germany,[9,10] France,[11] Austria,[12] Italy,[13,14] the United Kingdom,[15] Australia,[16] Brazil,[17] Korea,[18] Japan[19] and the United States.[20,21] *VCP* mutations have been noted in 2–3% of isolated familial ALS cases,[22] and 10–15% of individuals with hereditary inclusion body myopathy have an ALS-like phenotype characterized as a progressive neurodegenerative disease, involving both upper motor neurons and lower motor neurons.[5]

Recently, VCP has also shown to play a critical role in maintaining mitochondrial quality and dynamics in the PINK1/Parkin pathway, whereby pathogenic mutations in *VCP* lead to a block in proteasome-dependent degradation.[23] Other studies have demonstrated the autophagic mechanism of VCP regulation and function, an important process in

[1]Division of Genetics and Genomics Medicine, Department of Pediatrics, and [2]Department of Pathology and Laboratory Medicine, University of California–Irvine, Irvine, CA 92697.

mediating protein degradation for terminally differentiated cells. Autophagy is responsible for degrading defective organelles and the bulk of cytoplasm during starvation. Recent studies have shown that sequestosome 1 (p62/*SQSTM1)* interacts with the autophagic effector protein, light chain 3 (LC3-I/II), to mediate the uptake of aggregated proteins. VCP is important for the retro-translocation of misfolded endoplasmic reticulum (ER) proteins, and failure in this activity results in defective ER-associated protein degradation and ER stress responses.[24] Interestingly, the *SQSTM1* gene, encoding p62/*SQSTM1*, is involved in the autophagy and apoptosis signaling cascades, and is responsible for approximately 10% of sporadic PDB and 50% of familial PDB. Mutations in p62/*SQSTM1* have also now been associated with ALS. Impaired autophagic degradation is also involved in Alzheimer's and Huntington's diseases, among other neurodegenerative disorders.[25–29]

Generation of tamoxifen-inducible Cre models has become the gold standard for determining gene function in mice by allowing the phenotypic analyses for selected tissues during embryonic development, thus providing a powerful platform to analyze the functions of genes and proteins physiologically *in vivo*. More recently, studies based on novel gene, cell, and drug therapies in patients have shown promising exon skipping strategies to treat muscular dystrophies such as Duchenne muscular dystrophy (DMD), Becker muscular dystrophy,[30,31] and in other autosomal dominant disorders, including neurofibromatosis type I, frontotemporal dementia-associated Parkinsonism, and fibrodysplasia ossificans progressive (FOP). In FOP patients, this technology is carried out by reducing the excessive activin receptor-like kinase 2 (ACVR1/ALK2).[32] Exon skipping in VCP disease is currently being pursued as an effective translational suppression technology to skip exons hoping to pave the way toward a possible therapeutic strategy. Herein, we report on a proof-of-principle technology using the transgenic Cre-ER$^{TM}$-VCP$^{R155H/+}$ mouse model, with the targeted excision of the *VCP* R155H mutation demonstrating amelioration of the typical phenotypic features observed in VCP-associated diseased patients.

## Materials and Methods

### *Ethics statement*

All experiments were done with the approval of the Institutional Animal Care and Use Committee of the University of California–Irvine (Protocol #2007-2716-2), and in accordance with the guidelines established by the National Institutes of Health (NIH). Animals were housed in the animal facility and were maintained under constant temperature (22°C) and humidity with a controlled 12:12 hr light–dark cycle. Animals were observed throughout the entire experimental process in order to ameliorate any pain and suffering. Mice were euthanized by $CO_2$ inhalation followed by cervical dislocation.

### *Generation and validation of the Cre-ER$^{TM}$-VCP$^{R155H/+}$ mouse model*

The VCP disease mouse model was generated in our laboratory as previously described.[33] Male R26Cre-ER transgenic mice (Jackson Laboratories, Bar Harbor, ME; Strain #004847) were obtained as a kind gift from Edward Monuki (University of California–Irvine, Irvine, CA) and crossed to females carrying the most common *VCP* gene mutation R155H. These R26CreER mutant mice have a tamoxifen-inducible Cre-mediated recombination system driven by the endogenous mouse *ROSA* promoter. When crossed with a strain containing a *loxP* site-flanked sequence of interest, this mutant is useful for generating tamoxifen-induced, Cre-mediated targeted deletions. The presence of the *Cre* gene (genotyping) was confirmed by PCR using the following primers: forward, Cre 5′–GCACTGATTTCGACCAGGTT; reverse, Cre 3′–GCTAACCAGCGTTTTCGTTC with 50 ng DNA per sample. The primers for the PCR and long-range PCR were as follows: forward, AGTTAGGTATGAGGCTT CCAG; reverse, TGATTGGCACTGAGTGTGGT (50 ng per sample). Age-matched and sex-matched littermates ($n = 8–10$) were used in every experiment.

### *Induction of Cre activity with tamoxifen*

Tamoxifen (T5648; Sigma, St. Louis, MO) was dissolved in 5 ml of corn oil (Sigma) in a scintillation vial at 42°C for 30 min. Tamoxifen administration induces Cre recombination in the developing embryos of treated mouse dams; hence, pregnant Cre-ER$^{TM}$-VCP$^{R155H/+}$ females were treated with tamoxifen at 0.12 mg/g body weight or corn oil control by oral gavage (22-gauge feeding needle) at E6.75 once. Pups were monitored on a weekly basis, and weight and grip strength measurements were recorded as described previously.[34]

### *Measurements of weight and muscle strength*

Muscle strength of the forelimbs of Cre-ER$^{TM}$-VCP$^{R155H/+}$ and WT mice was measured by a Grip Strength Meter apparatus (TSE Systems Gmbh, Hamburg, Germany). Mice were held from the tip of the tail above the grid and gently lowered down until the front paws grasped the grid. Hind limbs were kept free from contact with the grid. The animal was brought to an almost horizontal position and pulled back gently but steadily until the grip was released. The maximal force achieved by the animal was recorded.

### *Confirmation of recombination by PCR*

Quadriceps, liver, kidney, and brain samples were harvested from the WT and Cre-ER$^{TM}$-VCP$^{R155H/+}$ mice to assess recombination following tamoxifen administration. Genomic DNA was purified from these tissues using the Qiagen DNeasy Blood & Tissue Kit following the manufacturer's instructions (Qiagen, Valencia, CA). Cre-mediated recombination was determined by PCR using the primers flanking the *loxP* sites: forward, 5′-AGTTAGGT ATGAGGCTTCCAG; reverse, 5′-TGATTGGCACTGAGT GTGGT. The PCR conditions were as follows: step 1, 95°C for 2 min; step 2, 95°C for 30 sec; step 3, 55°C for 30 sec; step 4, 72°C for 1 min; and then repeat steps 2–4 for 35 cycles and finally keep at 72°C for 5 min. Recombination of the *VCP* gene resulted in a deletion of 1,500 bp (exons 4 and 5), thus resulting in a smaller distance (500 bp) between the primers. Successful recombination resulted in 550 bp band detection by gel electrophoresis. This band was not observed in wild-type (WT) tamoxifen-treated or untreated mice.

*Efficiency of recombination by Q-PCR*

To confirm the efficiency of recombination, Q-PCR was used to detect the nonrecombined allele. Genomic DNA from quadriceps, liver, brain, and kidneys of WT and Cre-ER$^{TM}$-VCP$^{R155H/+}$ mice were purified from these tissues using the Qiagen DNeasy Blood & Tissue Kit following the manufacturer's instructions (Qiagen). The Q-PCR conditions were as follows: step 1, 95°C for 2 min; step 2, 95°C for 30 sec; step 3, 55°C for 30 sec; step 4, 72°C for 1 min; and then repeat steps 2–4 for 35 cycles and finally keep at 72°C for 5 min.

The primers (specific to the mouse mutant allele only) for this Q-PCR were as follows—primers for both excised and nonexcised products: CTTCGTATAGCATACATTATACG AA—forward (Het.Cre.control.F), ACACTCAGTGCCAATC ATTT—reverse (Het.Cre.control.R), and product = 153 bp; primers for excised only: GCCCGGCCAGAGATTATTA AT—forward (Het.Cre.excised.F), GTCCGAAGAACGGATC CAA—reverse (Het.Cre.excised.R), and product = 151 bp; primers for nonexcised only: CACTCAGGTAGTATTCATG TTGT—forward (Het.Cre.non-excised.F), TAGACTAATAC GCGTGGAC—reverse (Het.Cre.non-excised.R), and product = 151 bp. This analysis assessed the effectiveness of the Cre tamoxifen recombination in these different tissue types. For these Q-PCRs, one detected excised transcripts (eT) and one detected unexcised transcripts (uT). The following calculations were then used to determine efficiency: eT/tT × 100 = Total unexcised. uT/tT × 100 = Total excised. These two numbers totaled would be between 97% and 101%, showing it to be an efficient method to calculate total excised transcripts. The total mutant primers were used as the internal control to normalize, as the amount of excised and nonexcised was calculated relative to this transcript. Future analysis will also focus on the excision efficiency in osteoblasts/osteoclasts.

*Histological analysis*

Forelimb muscles were flash-frozen in isopentane cooled in liquid nitrogen, and brains from 18-month-old Cre-ER$^{TM}$-VCP$^{R155H/+}$ mice were harvested and embedded in OCT compound cryo-sectioning mounting media (Electron Microscopy Sciences, Hatfield, PA) and stored at −80°C before sectioning 10 $\mu$m sections. For brain harvesting, Cre-ER$^{TM}$-VCP$^{R155H/+}$ mice were perfused with 4% paraformaldehyde and sequentially transferred through several sucrose gradients, embedded, and sectioned. For immunohistochemical analyses, quadriceps and/or brain sections were incubated with anti-TDP-43-, ubiquitin-, glial fibrillary acidic protein (GFAP)-, HT7 (tau)-, VCP-, p62/*SQSTM1*-, and LC3-I/II-specific antibodies overnight in a humidified chamber. All primary antibodies were purchased from Abcam (Cambridge, MA). Monoclonal anti-alpha-tubulin (mouse IgG1 isotype) was derived from the hybridoma produced by the fusion of mouse myeloma cells and splenocytes from an immunized mouse. Purified chick brain tubulin was used as the immunogen. The isotype was determined by a double-diffusion immunoassay (Sigma-Aldrich, St. Louis, MO). Subsequently, sections were washed with TBST (0.5%) and incubated with fluorescein-conjugated secondary antibodies (Sigma-Aldrich) for 1 hr at room temperature and mounted with DAPI-containing mounting media (Vector Laboratories, Inc., Burlingame, CA). Sections were analyzed by fluorescence microscopy using an AxioVision image capture system (Carl Zeiss, Thornwood, NY). The number of animals used in each group was $n = 8$–10/group, and they were imaged and analyzed by an unbiased blinded personnel.

*Protein expression studies*

Quadriceps muscle and brain samples from 18-month-old tamoxifen-treated or corn oil (vehicle)-treated WT and Cre-ER$^{TM}$-VCP$^{R155H/+}$ mice were harvested and extracted using the NE-PER Nuclear and Cytoplasmic Extraction Kit (Thermo Scientific, Rockford, IL). Protein concentrations were determined using the Nanodrop according to the manufacturer's protocols. Equal amounts of proteins were separated on Bis-Tris 4–12% NuPAGE gels using the Novex Mini Cell (Invitrogen Life Technologies, Carlsbad, CA) according to manufacturer's protocols. The expression levels of proteins were analyzed by Western blotting: GAPDH (cytoplasmic-specific marker) (1:5,000); Histone H1 (nuclear-specific marker) (1:1,000); GFAP (1:500); HT7 (1:1,000); NeuN (1:500); VCP (1:2,000); TDP-43 (1:1,000); LC3-I/II (1:1,000); ubiquitin (1:1,000); p62/SQSTM1 (1:1,000); BAX (1:1,000); Bcl-2 (1:1,500); p53 upregulated modulator of apoptosis (PUMA; 1:2,000); alpha-tubulin (1:10,000); or $\beta$-actin (1:10,000) for equal loading. These experiments are representative of triplicates. Densitometry was performed to quantitate the Western blot bands using ImageJ Program (National Institutes of Health, Bethesda, MD).

*Assessment of oxidative mitochondrial markers*

Histochemical analyses and activity levels with succinic dehydrogenase (SDH; Sigma-Aldrich) and nicotinamide adenine dinucleotide (NADH; Sigma-Aldrich) were performed on quadriceps muscles from the Cre-ER$^{TM}$-VCP$^{R155H/+}$ and WT mice. Quadriceps cross sections were incubated with SDH or NADH for 2 hr in the incubator at 37°C. Following incubation, slides were cooled off for 5 min at room temperature and mounted with Aqua-mount (Thermo Scientific). The staining intensity of each slide was evaluated using light microscopy. Multivariate analyses were performed on SDH and NADH markers among treated and untreated WT and VCP$^{R155H/+}$ groups.

*TUNEL assay*

To measure apoptosis after 24 hr, TUNEL assay (Promega, Madison, WI) was performed per manufacturer's instructions. Briefly, slides were fixed in 4% paraformaldehyde for 15 min, washed in PBS for 5 min, and permeabilized with 20 $\mu$g/ml Proteinase K solution for 10 min at room temperature. Cells were then washed in PBS for 5 min, and 100 $\mu$l of equilibration buffer was added for 10 min. The cells were labeled with 50 $\mu$l of TdT reaction mix and incubated for 60 min at 37°C in a humidified chamber. Stop reaction was added for 15 min after which the cells were washed, counterstained, and prepared for analysis. The percentage of TUNEL-positive cells was calculated by counting all cells per slide. These experiments are representative of triplicates.

*Micro-computed tomography imaging*

Micro-computed tomography (microCT) scans were performed by scanning the WT and Cre-ER$^{TM}$-VCP$^{R155H/+}$ mice with a large-area CT camera. The reconstructed

microCT images were analyzed, and trabecular structural parameters were determined using the Inveon Multi-modality 3D Visualization software as previously described.[33]

### *Statistical analysis*

Means were used as summary statistics for all experiments. We compared the above studies—including muscle grip strength measurements, immunohistological, TUNEL studies, and densitometries—among tamoxifen- and corn oil control (vehicle)-treated WT and Cre-ER$^{TM}$-VCP$^{R155H/+}$ mice using mixed model analysis of variance (ANOVA), multivariate analyses (performed on SDH/NADH stainings among treated/untreated WT and VCP$^{R155H/+}$ groups), and pair-wise *t*-tests. Randomized samples were analyzed in 50 areas from 20 different slides.

## Results

### *Generation of Cre-recombinase tamoxifen-inducible VCP$^{R155H/+}$ mice*

The VCP$^{R155H/+}$ heterozygous mouse was created with two *loxp* sites, placed on either side of the R155H mutation in exons 4 and 5, allowing the possibility of deleting this region, thereby knocking the mutant allele out of frame, with Cre-*loxP* technology.[33] The rationale for deletion of exons 4 and 5 was to disrupt the mutant VCP open reading frame, thereby leaving the normal allele intact, providing proof of principle that removal of the mutated gene could result in amelioration of muscle pathology (Fig. 1a). In this investigation, we have crossed our VCP$^{R155H/+}$ mice with another mouse line containing the Cre-ER hybrid recombinase transgene, ubiquitously expressed in all tissues, driven by the endogenous mouse *ROSA* promoter, thereby generating a unique Cre-ER$^{TM}$-VCP$^{R155H/+}$ mouse model.

### *Administration of tamoxifen to pregnant females allows recombination during prenatal development*

We evaluated the effects of inducing Cre-mediated recombination during early postnatal development and postulated that oral gavage would rapidly induce Cre recombinase activity and have less toxicity than with intraperitoneal (i.p.) injections. Administration of tamoxifen to young pups by i.p. injection was found to be lethal in our studies similar to the findings by Furukawa et al.[35] The pregnant Cre-ER$^{TM}$-VCP$^{R155H/+}$ dams were oral gavaged once with tamoxifen (0.12 mg/g body weight) at E6.75, where the tamoxifen was transferred to the pups through the placental barrier.[35] Prenatal treatment was preferred as this allowed us to follow the effects of the mutation excision from an early age of development. Recombination was confirmed by PCR analysis (Fig. 1b) and Q-PCR analysis (Fig. 1c). Tamoxifen's half-life is 12 hr in mice, although the *in utero* effect may be permanent. Upon birth, the pups were monitored for weight and muscle strength measurements, up to 18 months of age.

### *Efficient and functional recombination by Q-PCR analysis*

We assessed the efficiency and functionality of Cre recombination in the pups of the tamoxifen-treated pregnant

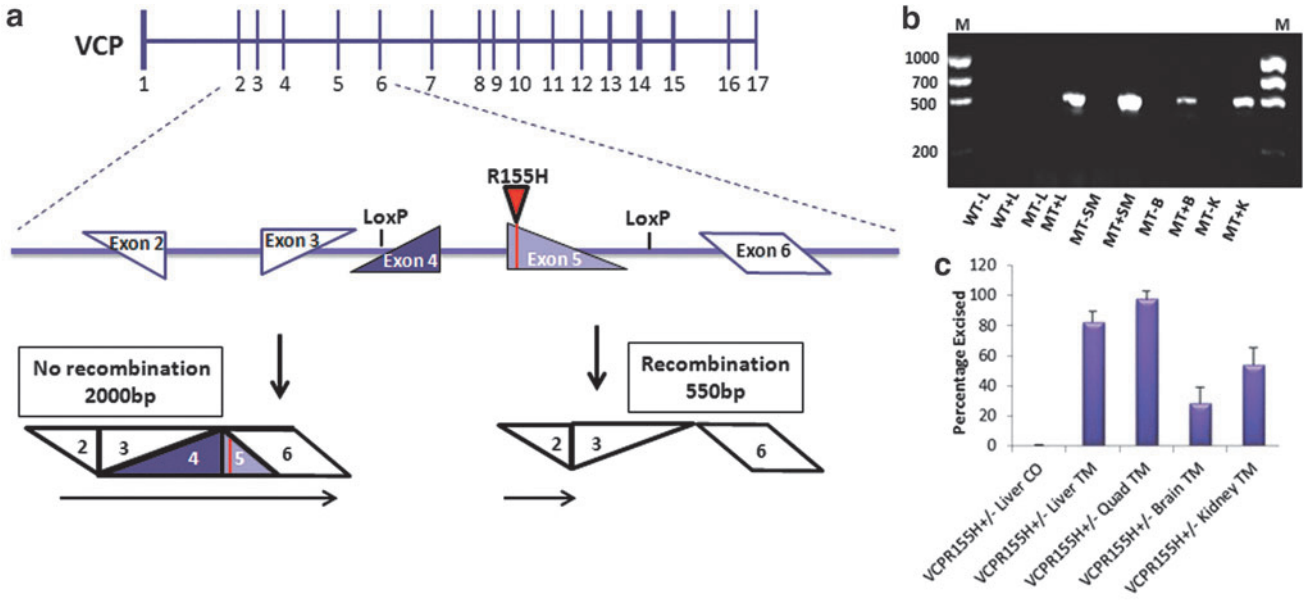


**FIG. 1.** Cre-mediated recombination and functionality in Cre-ER$^{TM}$-VCP$^{R155H/+}$ mice. **(a)** Schematic of exons 1–5 in the *VCP* gene with the R155H mutation flanked by *loxp* sites. **(b)** PCR analysis with primers flanking the *loxp* sites reveals 550 bp product after Cre-*loxp* recombination in the Cre-ER$^{TM}$-VCP$^{R155H/+}$ 3-week-old pups from Cre-ER$^{TM}$-VCP$^{R155H/+}$ pregnant mice. Lanes—M: molecular weight markers; WT-L, wild-type corn oil (CO)-treated (liver); 2: WT ± L, tamoxifen-treated (liver); 3: (mutant) MT-L, VCP$^{R155H/+}$ corn oil-treated (liver); 4: MT ± L, Cre-ER$^{TM}$-VCP$^{R155H/+}$ (liver); 5: MT-SM, VCP$^{R155H/+}$ corn oil-treated (skeletal quadriceps); 6: MT ± SM, Cre-ER$^{TM}$-VCP$^{R155H/+}$ (skeletal quadriceps); 7: MT-B, VCP$^{R155H/+}$ corn oil-treated (brain); 8: MT ± B, Cre-ER$^{TM}$-VCP$^{R155H/+}$ (brain); 9: MT-K, VCP$^{R155H/+}$ corn oil-treated (kidney); 10: MT ± K, Cre-ER$^{TM}$-VCP$^{R155H/+}$ (kidney). The number of animals used was $n = 10$/group. **(c)** Q-PCR analysis validated recombination efficiency in livers, quadriceps, brains, and kidneys from Cre-ER$^{TM}$-VCP$^{R155H/+}$ and WT mice. VCP, valosin-containing protein; WT, wild-type. Color images available online at www.liebertpub.com/hgtb

$VCP^{R155H/+}$ mice. The Cre-ER hybrid recombinase is trapped in the cellular cytoplasm and is unable to mediate recombination of the DNA region flanked by *loxP* sites until its activation with tamoxifen. Once tamoxifen is administered and binds to the murine estrogen receptor, Cre protein translocates to the nucleus to induce site-specific recombination.[34,36] The specificity of Cre recombinase was tested by immunohistochemistry using an anti-Cre-antibody (data not shown). The undeleted region results in a 2000 bp product (data not shown). PCR primers flanking the *loxp* sites give rise to a 550 bp PCR product when the region is deleted, confirming efficient Cre-mediated recombination of the *VCP* gene in the Cre-$ER^{TM}$-$VCP^{R155H/+}$ pups in liver, skeletal muscle, brain, and kidney samples (Fig. 1b). The band running slightly lower was confirmed to be nonspecific by sequencing (data not shown). Sequencing of PCR transcripts confirmed that exons 4 and 5 have selectively been removed to produce a truncated VCP transcript. This VCP transcript is 691 bp with the corresponding predicted protein size of 33.33 kDA, most likely resulting in the degradation of the mutant VCP protein. Excision efficiency of the Cre recombination was assessed by Q-PCR in liver (80%), quadriceps (90%), brain (25%), and kidney (50%) samples from Cre-$ER^{TM}$-$VCP^{R155H/+}$ mice as compared with the control corn oil $VCP^{R155H/+}$ mice (Fig. 1c).

### *Improvement of muscle strength and histology in Cre-$ER^{TM}$-$VCP^{R155H/+}$ mice*

$VCP^{R155H/+}$ mice have an equal life span to WT littermates.[37] Survival did not differ between the monitored tamoxifen-treated and untreated Cre-$ER^{TM}$-$VCP^{R155H/+}$ mice. Weight measurements of tamoxifen-treated and untreated WT and $VCP^{R155H/+}$ pups at 3, 9, 15, and 18 months of age did not show any significant differences (Fig. 2a). We next performed grip strength measurements to examine the effects of tamoxifen-induced Cre-mediated recombination on the muscle strength of Cre-$ER^{TM}$-$VCP^{R155H/+}$ transgenic mice. Remarkably, there was significant improvement in the muscle strength measurements in Cre-$ER^{TM}$-$VCP^{R155H/+}$ mice when compared with their control littermates at 15 and 18 months of age ($p < 0.05$). Specifically, grip strength analyses in Cre-$ER^{TM}$-$VCP^{R155H/+}$

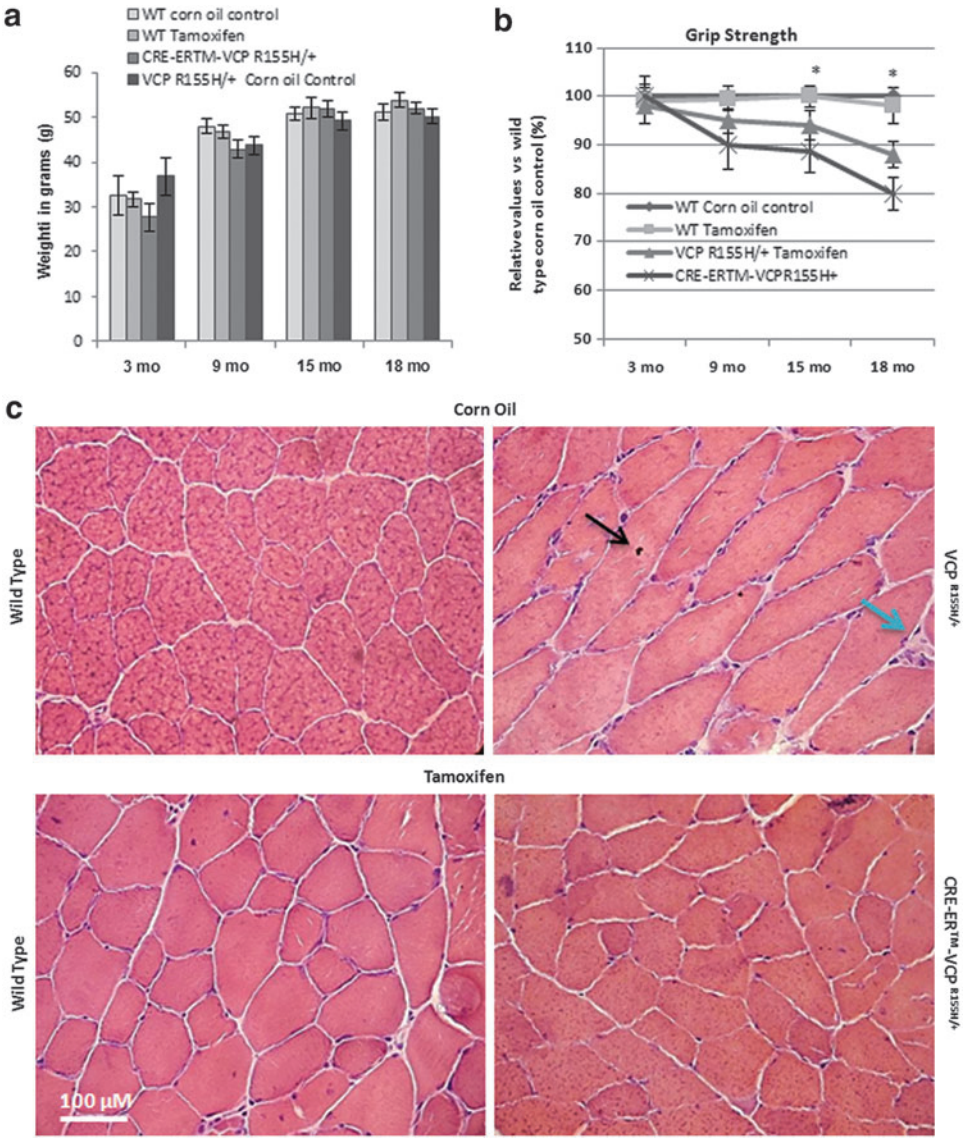


**FIG. 2.** Weight, grip strength, and histological analyses of Cre-mediated recombination in Cre-$ER^{TM}$-$VCP^{R155H/+}$ mice. **(a)** Weight analysis and **(b)** grip strength measurements of WT and Cre-$ER^{TM}$-$VCP^{R155H/+}$ tamoxifen-treated animals at 3, 9, 15, and 18 months of age, respectively. Histological analyses by H&E in **(c)** corn oil control or tamoxifen-treated WT and Cre-$ER^{TM}$-$VCP^{R155H/+}$ mice. Black arrow indicates centralized nuclei and degenerating fibers (blue arrow). Scale bar represents 100 $\mu$m. Statistical significance is denoted by $*p < 0.05$. The number of animals used was $n = 8$–10/group. Color images available online at www.liebertpub.com/hgtb

Table 1. Quantification of Fiber Parameters in Corn Oil- and Tamoxifen-Treated Wild-Type and $VCP^{R155H/+}$ Animals

| *Observed organelles* | *Area ($mm^2$)* | *WT corn oil control* | *WT tamoxifen-treated* | *$VCP^{R155H/+}$ corn oil control* | *Cre-$ER^{TM}$-$VCP^{R155H/+}$* |
|---|---|---|---|---|---|
| Vacuoles | 112,351 | 0 | 1.0 | 13.01* ± 0.47 | 2.04* ± 0.15 |
| Centrally located nuclei | 112,351 | 1.08 ± 0.45 | 2.05 ± 0.38 | 14.01* ± 0.84 | 3.05* ± 0.17 |
| Total endomysial space | 112,351 | 133.34 ± 0.54 | 133.092 ± 0.14 | 147.602* ± 0.25 | 126.104* ± 0.41 |
| Neurodegenerative fibers | 112,351 | 0.35% ± 0.15 | 0.87% ± 0.57 | 11.62*% ± 0.49 | 0.54*% ± 0.33 |

*$p < 0.05$ is considered statistically significant.

mice showed a 50% (15-month-old animals [SD ±3.1]) and 40% (18-month-old mice [SD ±2.6]) reduction in muscle strength loss as compared with the control corn oil $VCP^{R155H/+}$ heterozygotes (Fig. 2b).

We next evaluated the effects of inducing Cre-mediated recombination in the quadriceps of Cre-$ER^{TM}$-$VCP^{R155H/+}$ mice and control littermates by histology. The changes in histology in the Cre-$ER^{TM}$-$VCP^{R155H/+}$ animals included an improvement in the organization of the muscle fibers at 18 months of age (Fig. 2c), reduced centrally localized nuclei, decreased endomysial space, and a decrease in neurodegenerative fibers as compared with corn oil-treated $VCP^{R155H/+}$ animals (black arrow shows centrally located nuclei; blue arrow shows increased endomysial space). Table 1 represents quantification of the observed histological data.

### *Cre-$ER^{TM}$-$VCP^{R155H/+}$ mice exhibit improvement of the autophagic cascade in quadriceps*

The autophagy cascade whereby long-lived proteins are degraded is of critical importance in understanding one of the possible underlying mechanisms in VCP disease. We have previously shown that the autophagy pathway is disrupted in patients' myoblasts and our $VCP^{R155H/+}$ mouse models.[33,37,38] To determine whether autophagic processes were altered in the quadriceps muscles in the Cre-$ER^{TM}$-$VCP^{R155H/+}$ and WT mice, we analyzed levels of autophagy markers, including ubiquitin, LC3-I/II, p62/*SQSTM1*, VCP, and TDP-43 by immunohistochemistry (Fig. 3a), Western blotting (Fig. 3b), and densitometric analyses (Fig. 3c). Cre-$ER^{TM}$-$VCP^{R155H/+}$ mice revealed decreased protein expression levels of the autophagic markers, LC3-I/II and p62/*SQSTM1*, thereby suggesting

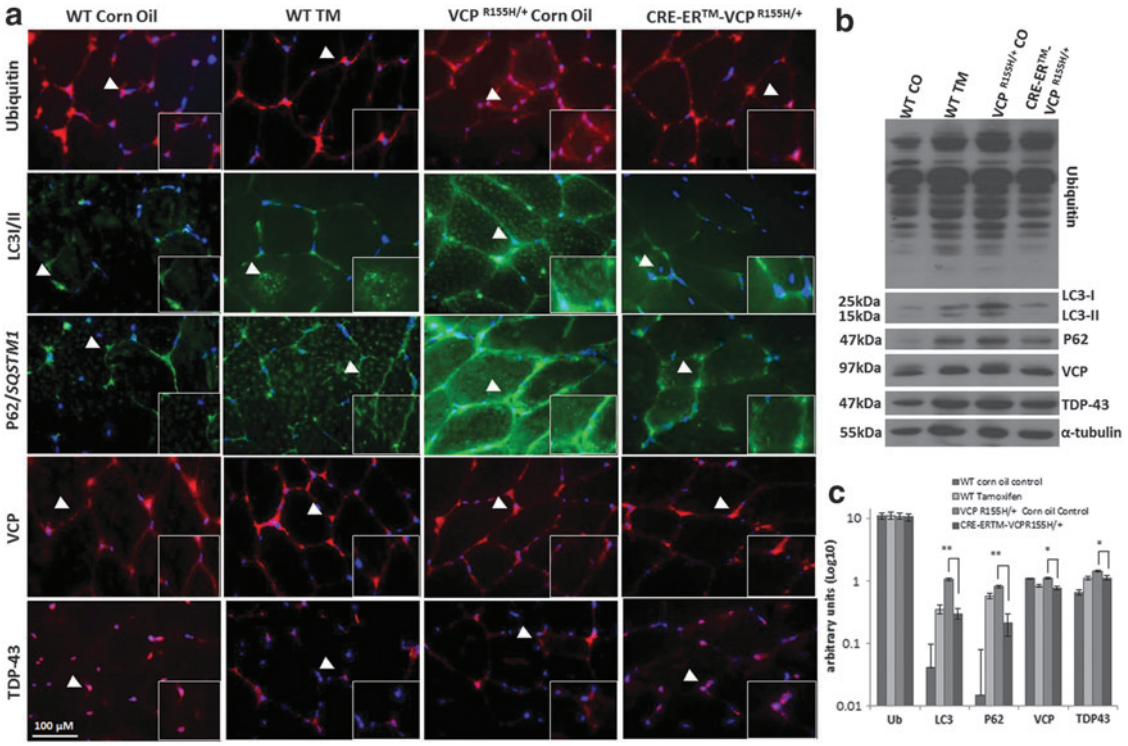


**FIG. 3.** Analysis of autophagy cascade in the quadriceps of Cre-$ER^{TM}$-$VCP^{R155H/+}$ and WT mice. Immunohistochemical analysis of **(a)** ubiquitin-, LC3-I/II-, p62/*SQSTM1*-, VCP-, and TDP-43-specific autophagy markers in quadriceps from 18-month-old WT and Cre-$ER^{TM}$-$VCP^{R155H/+}$ corn oil- and tamoxifen-treated animals, respectively. Scale bar represents 100 $\mu$m. Arrows indicate enlarged insets. **(b)** Western blot analysis of autophagy intermediates in 18-month-old WT and Cre-$ER^{TM}$-$VCP^{R155H/+}$ tamoxifen-treated animals. Alpha tubulin was used as loading controls. **(c)** Densitometric analysis of Western blots. Statistical significance is denoted by *$p < 0.05$ and **$p < 0.005$ with one-way ANOVA. The number of animals used was $n = 3$/group. Color images available online at www.liebertpub.com/hgtb

correction of the autophagic cascade, compared with corn oil (vehicle) $VCP^{R155H/+}$ mice (location of magnified insets are shown by white arrows) (Fig. 3a–c). However, ubiquitin was not significantly changed. Cre-$ER^{TM}$-$VCP^{R155H/+}$ mice depicted TDP-43 punctates in the nuclei and reduced cytoplasmic translocation of TDP-43 as compared with the control corn oil (vehicle) $VCP^{R155H/+}$ mice. Tamoxifen has been shown to be an autophagy and apoptosis inducer,[39] and thus levels of LC3-I/II and p62/*SQSTM1* autophagy markers were increased in WT mice treated with tamoxifen (Fig. 3b) as compared with control oil WT animals. Tamoxifen treatment did not have any effect on $\beta$-actin levels. All data were normalized to $\beta$-actin levels.

### *Decreased apoptotic cells by TUNEL in quadriceps Cre-$ER^{TM}$-$VCP^{R155H/+}$ mice*

Mutations in the *VCP* gene have been shown to trigger cell death by apoptosis. TUNEL analysis of the quadriceps muscles from the Cre-$ER^{TM}$-$VCP^{R155H/+}$ depicted a significant decrease in TUNEL+ cells by immunohistochemical methods (as shown by white arrows) (Fig. 4a) and quantification (Fig. 4b), suggesting important differences in apoptotic levels as compared with the corn oil (vehicle) control Cre-$ER^{TM}$-$VCP^{R155H/+}$ mice. To further explore the apoptotic cascade, we analyzed three anti- and pro-apoptotic markers, namely, Bcl-2, BAX, and the PUMA, and confirmed our expectations (Fig. 4c). There was increased expression in anti-apoptotic protein Bcl-2 between the tamoxifen-treated Cre-$ER^{TM}$-$VCP^{R155H/+}$ mice versus corn oil (vehicle)-treated Cre-$ER^{TM}$-$VCP^{R155H/+}$ mice (Fig. 4c). There was decreased expression of Bcl-2-associated X protein, BAX, and PUMA in the Cre-$ER^{TM}$-$VCP^{R155H/+}$ mice versus the corn oil (vehicle) mice (Fig. 4c); however, levels of the BAX protein were increased in the WT tamoxifen-treated animals possibly because of tamoxifen toxicity. Densitometry for these Western blots confirmed these results (Fig. 4d). Tamoxifen has been shown to be an autophagy and apoptosis inducer[39]; thus, it was expected to observe a slight increase in protein levels in tamoxifen-treated WT animals. Though the metabolism of tamoxifen is different in the mouse, rat, and human cancer patients, there is a permanent effect observed throughout each mouse's lifetime. The increases in tamoxifen-treated WT mice were statistically significant compared with their WT littermates (corn oil).

### *Mitochondrial enzymes are stimulated in Cre-recombinase $VCP^{R155H/+}$ mice*

To analyze the effects of tamoxifen-induced Cre recombinase activity on the mitochondrial complexes of Cre-$ER^{TM}$-$VCP^{R155H/+}$ and WT animals, we performed mitochondrial enzyme assays using SDH and NADH stains. Identification of oxidative and nonoxidative fibers by SDH staining is used in assessing mitochondrial pathology, where increased mitochondrial proliferation is indicative of mitochondrial dysfunction, as mitochondrial-rich type I fibers stain darker than anaerobic type II fibers. $VCP^{R155H/+}$ 18-month-old animals treated with corn oil demonstrated dark-stained angular-shaped atrophic type I fibers (as indicated by white arrows) compared with corn oil-treated WT littermates, which depicted a normal ''checkered'' pattern with NADH and SDH staining (Fig. 5a). In contrast, Cre-$ER^{TM}$-$VCP^{R155H/+}$ animals demonstrated a decrease in

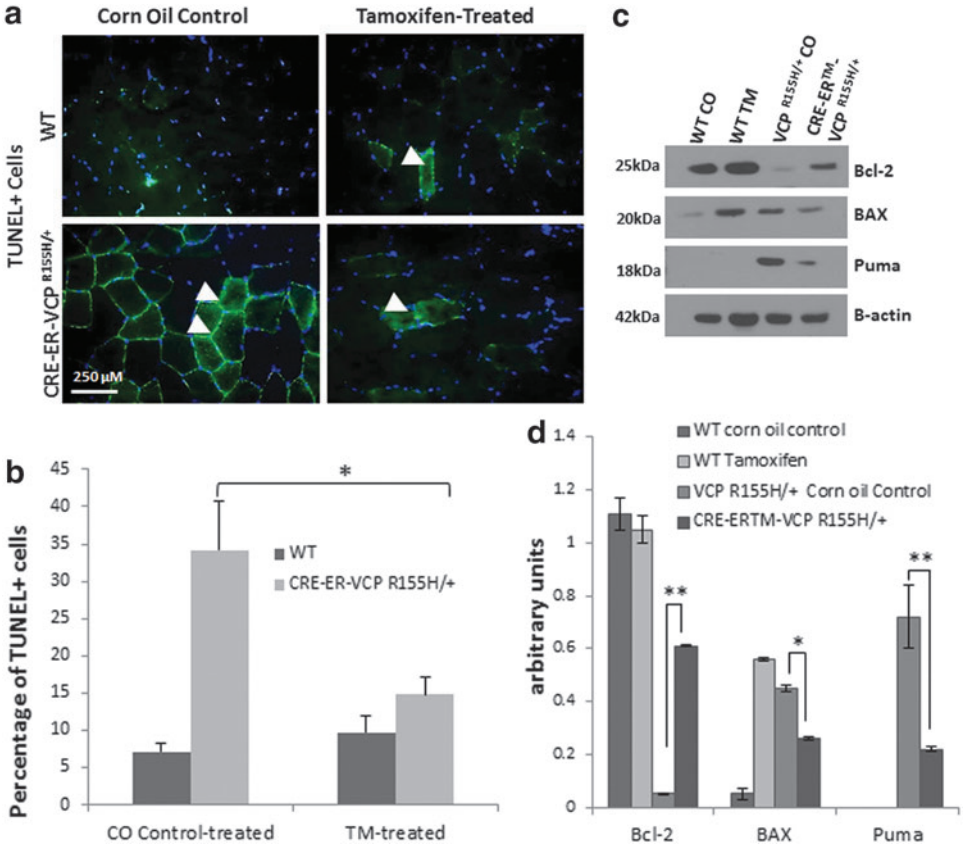


**FIG. 4.** TUNEL analyses of quadriceps of Cre-mediated recombination from Cre-$ER^{TM}$-$VCP^{R155H/+}$ mice. TUNEL staining of quadriceps muscles from corn oil (CO)-treated **(a)** WT and Cre-$ER^{TM}$-$VCP^{R155H/+}$ mice, and tamoxifen (TM)-treated WT and $VCP^{R155H/+}$ mice at 18 months of age (magnification: 630×). Arrows indicate TUNEL+ cells. Scale bar represents 250 $\mu$m. **(b)** Quantification of TUNEL+ cells in corn oil (vehicle)- and tamoxifen-treated Cre-$ER^{TM}$-$VCP^{R155H/+}$ mice. **(c)** Western blot analysis of apoptosis markers, Bcl-2, BAX, and Puma in 18-month-old WT and Cre-$ER^{TM}$-$VCP^{R155H/+}$ tamoxifen-treated animals. $\beta$-Actin was used as a loading control for these samples. **(d)** Densitometry analysis confirmed levels of the apoptosis markers. Statistical significance is denoted by $*p < 0.05$ and $**p < 0.005$ with one-way ANOVA. The number of animals used was $n = 3$/group. Color images available online at www.liebertpub.com/hgtb

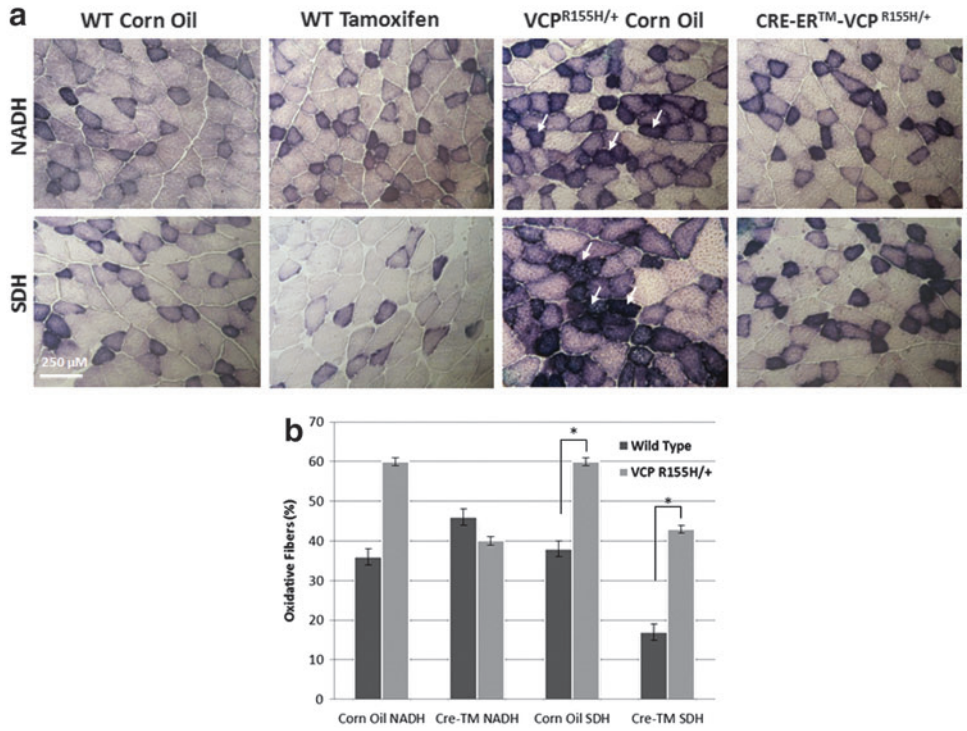


**FIG. 5.** Mitochondrial enzyme analysis of Cre-ER$^{TM}$-VCP$^{R155H/+}$ mice. Staining with **(a)** NADH and SDH in WT and Cre-ER$^{TM}$-VCP$^{R155H/+}$ corn oil control (vehicle)- and tamoxifen-treated animals, respectively. **(b)** Quantification of SDH and NADH oxidative fibers in WT and Cre-ER$^{TM}$-VCP$^{R155H/+}$ corn oil control (vehicle)- and tamoxifen-treated animals. Scale bar represents 250 $\mu$m. Statistical significance is denoted by $*p<0.05$. The number of animals used was $n=8$–10/group. Color images available online at www.liebertpub.com/hgtb

type I fibers, suggestive of a reduction in mitochondrial pathology (Fig. 5a). A decrease in SDH staining was observed in the tamoxifen-treated WT animals possibly because of tamoxifen toxicity; however, it was not significant (Fig. 5a). Quantification of NADH and SDH oxidative fibers in control and tamoxifen-treated WT and Cre-ER$^{TM}$-VCP$^{R155H/+}$ animals confirmed these findings ($p<0.05$), demonstrating a 10% reduction in WT and a 20% reduction in tamoxifen-treated NADH-stained oxidative fibers as compared with control corn oil VCP$^{R155H/+}$ animals (Fig. 5b). Similarly, tamoxifen-treated WT animals showed a 20% reduction in oxidative fibers and Cre-ER$^{TM}$-VCP$^{R155H/+}$ animals depicted an 18% decrease in SDH-stained fibers compared with control corn oil VCP$^{R155H/+}$ animals.

### *Improvement of frontal cortex pathology by autophagy cascade in Cre-ER$^{TM}$-VCP$^{R155H/+}$ mice*

We evaluated the autophagy cascade in the cytoplasmic and nuclear frontal cortex extracts from control corn oil (vehicle) and tamoxifen-treated WT and VCP$^{R155H/+}$ heterozygote mice by immunohistochemistry (location of magnified insets is shown by white arrows) (Fig. 6a) and Western blotting analyses (Fig. 6b). There were no significant differences noted between the cytoplasmic and nuclear protein lysates from the control corn oil (vehicle)- and tamoxifen-treated WT and VCP$^{R155H/+}$ samples for GFAP, a marker of astrocyte proliferation, LC3-I/II, p62/*SQSTM1* and ubiquitin, autophagy markers, and VCP protein levels (Fig. 6b). Differences were observed between cytoplasmic and nuclear brain protein extracts from control corn oil (vehicle)- and tamoxifen-treated WT and VCP$^{R155H/+}$ samples for HT7 (tau), a marker of neurodegeneration, NeuN, and TDP-43 protein expression levels (Fig. 6b). Specifically, cytoplasmic levels of HT7 (tau), NeuN, and TDP-43 were increased in the corn oil control VCP$^{R155H/+}$ animals, whereas there were no changes in the nuclear extracts. Interestingly, Cre-ER$^{TM}$-VCP$^{R155H/+}$ animals depicted decreased levels of all three, HT7 (tau), NeuN, and TDP-43, suggestive of an improvement in frontal cortex pathology (Fig. 6a and b). Tamoxifen-treated WT levels depicted increased cytoplasmic HT7 (tau), possibly because of tamoxifen toxicity; however, ubiquitin and GFAP inclusions decreased (Fig. 6a and b). Densitometry levels of the immunoblots for the cytoplasmic and nuclear fractions confirmed these findings (Fig. 6c). The half-life of tamoxifen is 12 hr in the mouse; however, the metabolism differs among species with a permanent effect. $\beta$-Actin levels were used as a loading control among all the samples.

### *Improvement of Paget-like lesions in Cre-ER$^{TM}$-VCP$^{R155H/+}$ mice*

We characterized the bone pathology in the tamoxifen-treated and corn oil control Cre-ER$^{TM}$-VCP$^{R155H/+}$ and WT mice at 18 months of age by microCT imaging and histological techniques. Gross microCT images showed no significant skeletal differences in the corn oil control or Cre-ER$^{TM}$-VCP$^{R155H/+}$ mice (Fig. 7a and b); however, close inspection of the hind limb bones in the Cre-ER$^{TM}$-VCP$^{R155H/+}$ mice at 18 months of age demonstrated reduced formation of PDB-like lytic lesions (as shown by yellow arrows) (Fig. 7c and d). Of the five animals analyzed, four out of five corn oil-treated VCP$^{R155H/+}$ mice had PDB-like lytic lesions and one out of five tamoxifen-treated Cre-ER$^{TM}$-VCP$^{R155H/+}$ mice showed lytic lesions, suggesting amelioration of the PDB-like phenotype in these mice.

## Discussion

Specific disease mechanisms and novel therapeutic advancements underlying VCP-associated myopathies and neurodegenerative disorders are under further investigation. Evolutionarily,

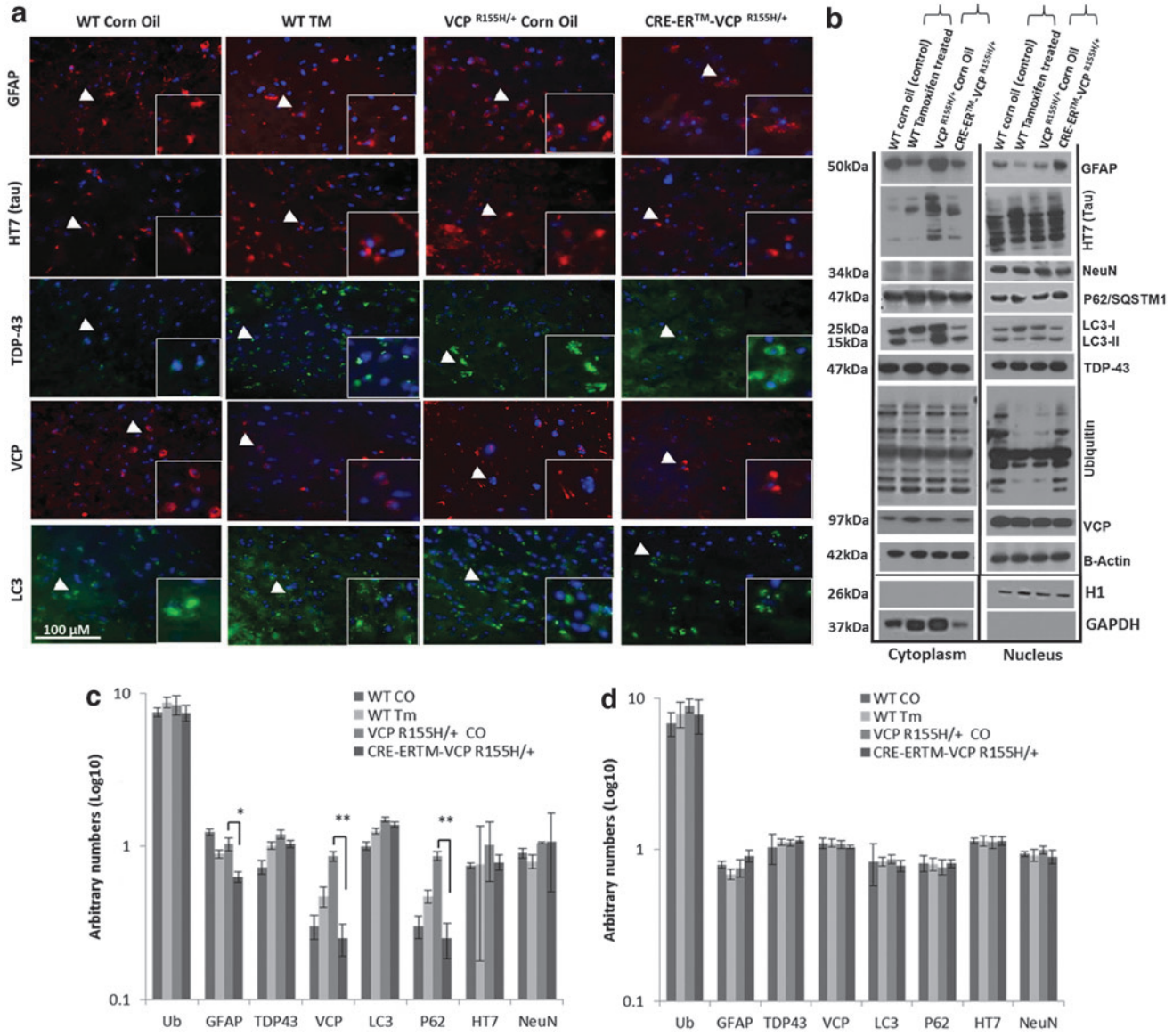


**FIG. 6.** Neuropathological frontal cortex analysis of autophagy cascade in Cre-ER$^{TM}$-VCP$^{R155H/+}$ mice. Immunohistochemical analysis of **(a)** GFAP, HT7 (tau), TDP-43, VCP, and LC3 protein expression levels in the frontal cortices from 18-month-old WT and Cre-ER$^{TM}$-VCP$^{R155H/+}$ corn oil- and tamoxifen-treated animals (magnification: 400×). Scale bar represents 100 $\mu$m. **(b)** Western blot analysis of GFAP, HT7 (tau), NeuN, P62, LC3-I/II, TDP-43, ubiquitin, VCP, $\beta$-actin, Histone H1, GAPDH, in 18-month-old WT and Cre-ER$^{TM}$-VCP$^{R155H/+}$ frontal cortices from tamoxifen-treated animals. Arrows indicate enlarged insets. **(c)** Densitometric analysis of the cytoplasm fraction confirmed findings of the Western blot. **(d)** Densitometric analysis of the nuclear fraction confirmed findings of the Western blot. Statistical significance is denoted by $^{*}p<0.05$ and $^{**}p<0.005$ with one-way ANOVA. $\beta$-Actin was used as a loading control. The number of animals used was $n=3$/group. Color images available online at www.liebertpub.com/hgtb

VCP is highly conserved and plays a significant role in several cellular processes in both unicellular and multicellular organisms. The knock-in VCP$^{R155H/+}$ mouse model exhibits progressive muscle weakness, and histological changes, including inclusions and vacuoles in the muscle fibers, Paget-like bone changes, and brain and spinal cord pathology of the human VCP disease, thereby providing a useful experimental platform to further investigate the mechanism(s) responsible for these VCP-associated disorders. Generation of conditional tamoxifen-inducible Cre-*loxP* mouse models has been utilized in a number of neuromuscular and degenerative diseases, including inducible androgen receptor knockout models, spinal muscular atrophy, muscular dystrophies including DMD, Alzheimer's disease, and ALS.[40] Recently, exon skipping as a therapeutic platform has demonstrated successful treatment in DMD mice and patients.[41–43]

Here, we describe our novel tamoxifen-inducible Cre-ER$^{TM}$-VCP$^{R155H/+}$ mouse line as a powerful tool and show that targeted excision of the R155H mutation in exons 4 and 5 ameliorates the phenotype typically observed in patients with VCP-associated disease. The rationale for deletion of exons 4 and 5 was to disrupt the mutant VCP open reading frame, thereby leaving the normal allele intact, providing proof of principle that removal of the mutated gene could result in the

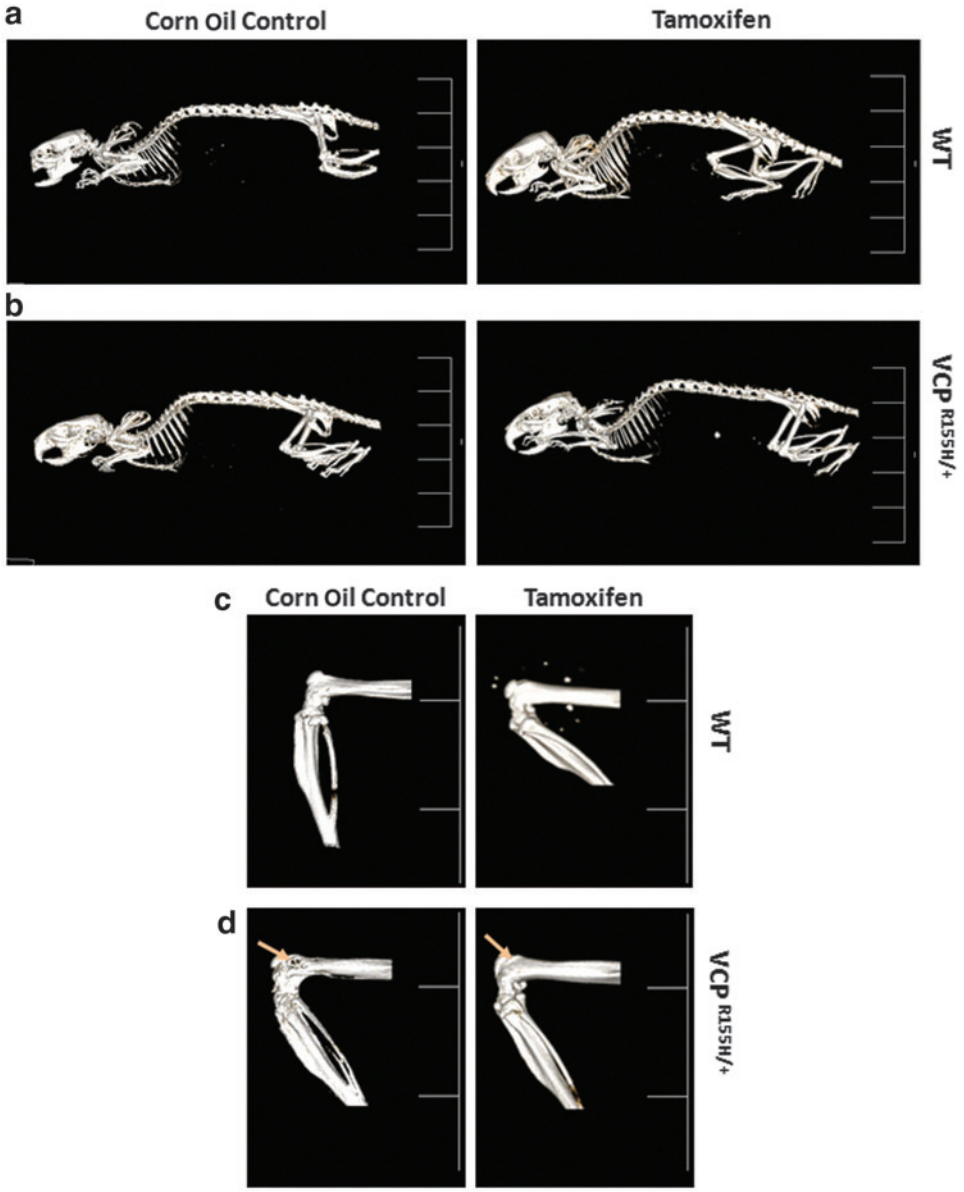


**FIG. 7.** (**a** and **b**) MicroCT analyses of hind limb bones in WT and Cre-ER$^{TM}$-VCP$^{R155H/+}$ mice. (**c** and **d**) Gross microCT images of hind limb bones in WT and Cre-ER$^{TM}$-VCP$^{R155H/+}$ mice. The number of animals used was $n = 8–10$/group. (**d**) Paget-like lytic lesion in VCP$^{R155H/+}$ control mouse is shown by an arrow in the left panel, whereas the tamoxifen-treated VCP$^{R155H/+}$ mouse depicted no lesions in the right panel. MicroCT, micro-computed tomography. Color images available online at www.liebertpub.com/hgtb

improvement of muscle and brain pathologies. The *Cre-loxP* recombination system cannot be currently used in humans because of technicalities in the manipulation of genes in a cell type-specific or inducible manner, but provides proof of principle. The emergence of exon skipping technology provides the advent of skipping exons with disease mutations, in this case, generating an ''out-of-frame'' shift, resulting in protein degradation. During processing of pre-mRNA, which is copied from the DNA template, introns are removed and exons are precisely spliced together to create the mature mRNA. By targeting elements in pre-mRNA that are essential for splicing, splice switching oligomers force the cellular machinery to skip over targeted exons, thereby creating an altered mRNA template, ultimately resulting in restored or neutralized protein by induced skipping of a specific exon. Current investigations are researching the development, optimization, and characterization of exon skipping oligonucleotide therapeutics in VCP disease patient myoblasts *in vitro* and subsequently *in vivo* in the VCP$^{R155H/+}$ heterozygote models.

In particular, when compared with the control corn oil (vehicle) Cre-ER$^{TM}$-VCP$^{R155H/+}$ mice, we discovered a significant improvement in muscle strength measurements by the grip strength test and partial amelioration of the typical pathology of VCP-associated disease. Furthermore, impaired autophagy has been observed in several human diseases, including myopathies and lysosomal storage disorders. Autophagy is a highly conserved mechanism, which is necessary for the maintenance of cellular homeostasis and orchestration of stress responses upregulated by oxidative stress, starvation, or other harmful conditions. Pro-LC3 is processed to its cytosolic form, LC3-1, exposing a carboxyl terminal Gly. LC3-1 is activated by Atg7, transferred to Atg3, a second E2-like enzyme, and modified to a membrane-bound form, LC3-II, which is localized to preautophagosomes and autophagosomes, making this protein an autophagosomal marker. Following the fusion of autophagosomes with lysosomes, intra-autophagosomal LC3-II is degraded by lysosomal hydrolytic enzymes. We found that Cre-ER$^{TM}$-VCP$^{R155H/+}$

animals had an improvement in the autophagy cascade by the decrease observed in the p62/*SQSTM1*, LC3-I/II, ubiquitin, and TDP-43 expression levels, possibly suggesting increased fusion between LC3-II-localized vesicles and lysosomes. Interestingly, a decrease in apoptotic cells and in the mitochondrial enzymes NADH and SDH in type I fibers was also detected, demonstrating a reduction in mitochondrial myopathy.

Frontotemporal dementia primarily affects the frontal and anterior temporal lobes of the brain with abnormalities in behavior, personality, and language. We observed decreased accumulation of TDP-43-, ubiquitin-, HT7 (tau)-, and GFAP-positive inclusions in the brains of 18-month-old Cre-ER$^{TM}$-VCP$^{R155H/+}$ tamoxifen-treated versus corn oil control mice. Also, the TDP-43-positive inclusions in the control corn oil (vehicle) VCP$^{R155H/+}$ mice were cytoplasmic, in contrast to the nuclear localization in the cortex and hippocampus of Cre-ER$^{TM}$-VCP$^{R155H/+}$ mice.

Paget disease of bone is usually characterized by osteoclastic lesions, abnormal bone remodeling, bone deformities, and pathologic fractures. The osteoclastic activity leads to resorption of bone and shortly thereafter by hyperactivity of the osteoblasts, leading to a disordered deposition of new bone resulting in Pagetic-like lesions. The lesions become sclerotic in the later stages of PDB and bone marrow is replaced with fibrous tissue and increased bone thickness. Studies have shown that 10% patients with sporadic PDB and 50% familial PDB have gene mutations of sequestosome 1 (*SQSTM1*). More recently, research has shown that p62/*SQSTM1* plays an important role in the autophagic cascade and knockout mouse models have demonstrated focal osteolytic lesions on the hind limbs. Close inspection of the long hind limb bones by microCT reveals lucencies of the proximal tibias of 18-month-old corn oil-treated Cre-ER$^{TM}$-VCP$^{R155H/+}$, suggestive of PDB. Our studies suggest that the Cre-*loxP* technology excision of the R155H mutation from the *VCP* gene results in a partial amelioration of PDB-like changes.

In the present study, it is not clear whether the amelioration observed through tamoxifen administration is primarily by a direct effect of tamoxifen or a secondary effect. In our studies, tamoxifen is having a permanent effect on the maturing pups, likely because of several properties of the drug, including its known ability to cross the blood–brain barrier. Tamoxifen is a weak anti-estrogen that undergoes extensive biotransformation in humans to metabolites that have far greater anti-estrogenic potency. 4-Hydroxytamoxifen (4-HT) represents less than 10% of Tamoxifen primary oxidation, but has 100-fold greater affinity for the estrogen receptor and 30–100-fold greater potency in suppressing estrogen-dependent cell proliferation compared with Tamoxifen.

This is the first report of the Cre-ER$^{TM}$-VCP$^{R155H/+}$ mice using the ROSA version of the recombinase of the human estrogen receptor and crossing it with the VCP$^{R155H/+}$ mice to generate a novel excised R155H DNA segment flanked by *loxP* sites. This provides proof of principle that removal of exons 4 and 5, resulting in amelioration of the VCP-associated disease phenotype, could be beneficial to patients. There are several novel techniques currently available that are being used in other diseases that could make this translational to VCP-associated disease patients. This article provides insight into exon splicing/skipping strategies in VCP-associated diseases and its translational therapeutic value for VCP patients. Cre-ER$^{TM}$-VCP$^{R155H/+}$ mice show improvements in the typical muscle pathology observed in the heterozygote mice carrying the R155H mutation. Although exon skipping has been used successfully in X-linked disorders such as DMD to produce a smaller functional protein, it has only rarely been utilized in autosomal dominant disorders by knockdown of the disease allele as reported in FOP.[32,41,43,44] Thus, the Cre-ER$^{TM}$-VCP$^{R155H/+}$ mouse conclusively serves as a highly valuable model for novel therapeutic strategies such as allele silencing for the human VCP-disease among other neurodegenerative genetic disorders.

## Acknowledgments

We wish to thank Tom Fielder, Kimberly Lank, Grant McGregor, Katrina Waymire, Gregory Chinn, Veeral Katheria, and Jennifer Chavez for their helpful discussions on the mice studies. We thank Drs. Cristian Constantinescu and Mohammad Reza Mirbolooki for technical assistance with the MicroCT. We thank Rebecca Mar-Heyming for technical assistance with the Q-PCR, and Naomi Walker and Arianna Gomez for the protein expression blots. Funding for this study was provided by NIH Grant AR050236 and Muscular Dystrophy Association MDA175682 to V.E.K.

## Author Disclosure Statement

The funders had no role in study design, data collection and analysis, decision to publish, or preparation of the article. No competing financial interests exist.

## References

1. Kimonis VE, et al. Clinical and molecular studies in a unique family with autosomal dominant limb-girdle muscular dystrophy and Paget disease of bone. Genet Med 2000; 2:232–241.
2. Kovach MJ, et al. Clinical delineation and localization to chromosome 9p13.3-p12 of a unique dominant disorder in four families: hereditary inclusion body myopathy, Paget disease of bone, and frontotemporal dementia. Mol Genet Metab 2001;74:458–475.
3. Watts GD, et al. Clinical and genetic heterogeneity in chromosome 9p associated hereditary inclusion body myopathy: exclusion of GNE and three other candidate genes. Neuromuscul Disord 2003;13:559–567.
4. Watts GD, et al. Inclusion body myopathy associated with Paget disease of bone and frontotemporal dementia is caused by mutant valosin-containing protein. Nat Genet 2004;36:377–381.
5. Kimonis VE, et al. Clinical studies in familial VCP myopathy associated with Paget disease of bone and frontotemporal dementia. Am J Med Genet A 2008;146:745–757.
6. Kimonis VE, et al. VCP disease associated with myopathy, Paget disease of bone and frontotemporal dementia: review of a unique disorder. Biochim Biophys Acta 2008;1782:744–748.
7. Kimonis VE, Watts GD. Autosomal dominant inclusion body myopathy, Paget disease of bone, and frontotemporal dementia. Alzheimer Dis Assoc Disord 2005;19:S44–S47.
8. Kimonis V, et al. Inclusion body myopathy associated with paget disease of bone and/or frontotemporal dementia gene. Muscle Nerve 2011. doi: 10.1002/mus.23960.
9. Schroder R, et al. Mutant valosin-containing protein causes a novel type of frontotemporal dementia. Ann Neurol 2005; 57:457–461.

10. Djamshidian A, et al. A novel mutation in the VCP gene (G157R) in a German family with inclusion-body myopathy with Paget disease of bone and frontotemporal dementia. Muscle Nerve 2009;39:389–391.
11. Guyant-Marechal L, et al. Valosin-containing protein gene mutations: clinical and neuropathologic features. Neurology 2006;67:644–651.
12. Haubenberger D, et al. Inclusion body myopathy and Paget disease is linked to a novel mutation in the VCP gene. Neurology 2005;65:1304–1305.
13. Bersano A, et al. Inclusion body myopathy and frontotemporal dementia caused by a novel VCP mutation. Neurobiol Aging 2007;30:752–758.
14. Viassolo V, et al. Inclusion body myopathy, Paget's disease of the bone and frontotemporal dementia: recurrence of the VCP R155H mutation in an Italian family and implications for genetic counselling. Clin Genet 2008;74:54–60.
15. Miller TD, et al. Inclusion body myopathy with Paget disease and frontotemporal dementia (IBMPFD): clinical features including sphincter disturbance in a large pedigree. J Neurol Neurosurg Psychiatry 2009;80:583–584.
16. Kumar KR, et al. Two Australian families with inclusion-body myopathy, Paget's disease of bone and frontotemporal dementia: novel clinical and genetic findings. Neuromuscul Disord 2010;20:330–334.
17. Fanganiello RD, et al. A Brazilian family with IBMPFD caused by p.R93C mutation in the VCP gene and literature review for genotype-phenotype correlations. Exp Brain Res 2011; 44:374–380.
18. Kim EJ, et al. Inclusion body myopathy with Paget disease of bone and frontotemporal dementia linked to VCP p.Arg155Cys in a Korean family. Arch Neurol 2011;68: 787–796.
19. Komatsu J, et al. Inclusion body myopathy with Paget disease of the bone and frontotemporal dementia associated with a novel G156S mutation in the VCP gene. Muscle Nerve 2013. [Epub ahead of print]; doi: 10.1002/mus.23960.
20. Watts GD, et al. Novel VCP mutations in inclusion body myopathy associated with Paget disease of bone and frontotemporal dementia. Clin Genet 2007;72:420–426.
21. Spina S, et al. Frontotemporal dementia associated with a valosin-containing protein mutation: report of three families. FASEB J 2008;22:58.4.
22. Johnson JO, et al. Exome sequencing reveals VCP mutations as a cause of familial ALS. Neuron 2010;68:857–864.
23. Kim NC, et al. VCP is essential for mitochondrial quality control by PINK1/Parkin and this function is impaired by VCP mutations. Neuron 2013;78:65–80.
24. DeLaBarre B, et al. Central pore residues mediate the p97/VCP activity required for ERAD. Mol Cell 2006;22: 451–462.
25. Wong E, Cuervo AM. Autophagy gone awry in neurodegenerative diseases. Nat Neurosci 2010;13:805–811.
26. Komatsu M, et al. Autophagy and neurodegeneration. Autophagy 2006;2:315–317.
27. Levine B, Kroemer G. Autophagy in the pathogenesis of disease. Cell 2008;132:27–42.
28. Malicdan MC, Nishino I. Autophagy in lysosomal myopathies. Brain Pathol 2012;22:82–88.
29. Tung YT, et al. Autophagy: a double-edged sword in Alzheimer's disease. J Biosci 2012;37:157–165.
30. Kemaladewi DU, et al. Dual exon skipping in myostatin and dystrophin for Duchenne muscular dystrophy. BMC Med Genomics 2011;4:36.
31. Pichavant C, et al. Current status of pharmaceutical and genetic therapeutic approaches to treat DMD. Mol Ther 2011;19:830–840.
32. Shi S, et al. Antisense-oligonucleotide mediated exon skipping in activin-receptor-like kinase 2: inhibiting the receptor that is overactive in fibrodysplasia ossificans progressiva. PLoS One 2013;8:e69096.
33. Badadani M, et al. VCP associated inclusion body myopathy and paget disease of bone knock-in mouse model exhibits tissue pathology typical of human disease. PLoS One 2010;5:e13183.
34. Zhang W, et al. Malignant glioma sensitivity to radiotherapy, high-dose tamoxifen, and hypericin: corroborating clinical response *in vitro*: case report. Neurosurgery 1996;38:587–590; discussion 590–591.
35. Furukawa S, et al. The impairment of metrial gland development in tamoxifen exposed rats. Exp Toxicol Pathol 2012;64:121–126.
36. Verrou C, et al. Comparison of the tamoxifen regulated chimeric Cre recombinases MerCreMer and CreMer. Biol Chem 1999;380:1435–1438.
37. Nalbandian A, et al. A progressive translational mouse model of human valosin-containing protein disease: the VCP(R155H/+) mouse. Muscle Nerve 2013;47:260–270.
38. Vesa J, et al. Valosin containing protein associated inclusion body myopathy: abnormal vacuolization, autophagy and cell fusion in myoblasts. Neuromuscul Disord 2009;19: 766–772.
39. de Medina P, et al. Tamoxifen and AEBS ligands induced apoptosis and autophagy in breast cancer cells through the stimulation of sterol accumulation. Autophagy 2009;5:1066–1067.
40. Kudoh H, et al. A new model mouse for Duchenne muscular dystrophy produced by 2.4 Mb deletion of dystrophin gene using Cre-loxP recombination system. Biochem Biophys Res Commun 2005;328:507–516.
41. Aoki Y, et al. Bodywide skipping of exons 45–55 in dystrophic mdx52 mice by systemic antisense delivery. Proc Natl Acad Sci USA 2012;109:13763–13768.
42. Malerba A, et al. Dual myostatin and dystrophin exon skipping by morpholino nucleic acid oligomers conjugated to a cell-penetrating peptide is a promising therapeutic strategy for the treatment of duchenne muscular dystrophy. Mol Ther Nucleic Acids 2012;1:e62.
43. Yang L, et al. Effective exon skipping and dystrophin restoration by 2′-o-methoxyethyl antisense oligonucleotide in dystrophin-deficient mice. PLoS One 2013;8:e61584.
44. Wu B, et al. Effective rescue of dystrophin improves cardiac function in dystrophin-deficient mice by a modified morpholino oligomer. Proc Natl Acad Sci USA 2008;105:14814–14819.

Address correspondence to:
*Dr. Virginia E. Kimonis*
*Division of Genetics and Genomics Medicine*
*Department of Pediatrics*
*University of California–Irvine*
*101 The City Drive South*
*Irvine, CA 92697*

*E-mail:* vkimonis@uci.edu

Received for publication July 30, 2014;
accepted after revision December 23, 2014.

Published online: December 29, 2014.